

Identifying adhesive components in a model tunicate

Fan Zeng, Julia Wunderer, Willi Salvenmoser, Thomas Ederth and Ute Rothbächer

Supplementary material

Suppl. Figure 1. Glycan profiling of *C. intestinalis* larvae: tunic (and test cells).

Lectin fluorescent labelling with: (A, A') GSL, (B, B') jacalin, (C, C') LCA, (D, D') SBA and (E, E') STL, (F, F') VVL, (G, G') LEL and (H, H') PSA. (A-H) Bright field and (A'-H') fluorescence images, respectively, anterior to the left. (F'-H'). Scale bar: 100 μ m.

Suppl. Figure 2. Glycan profiling of *C. intestinalis* larvae: notochord/nerve cord and nuclei.

Lectin fluorescent labelling on larvae with (A-A'') UEA I and (B-C'') EBL. (A') UEA I staining with the marked area (A'') enlarged, the arrow and arrowhead pointing to the notochord and the dorsal nerve cord, respectively. (B-B'') EBL fluorescence and (C-C'') EBL double fluorescence with nuclear DAPI showing the head/trunk region enlarged with (C) EBL staining, (C') DAPI staining and (C'') the complete overlap in nuclei. Anterior to the left. Scale bars: (A-A', B-B'') 100 μ m, (A'', C-C'') 50 μ m.

Suppl. Figure 3. Heparin mediated hydrophilic surface conversion.

Wetting properties on hydrophobic Petri dishes (from upper left to lower right) of ASWH, or heparin, glutamic acid and aspartic acid (each 2.5% in ASWH). 2 ml of the respective solutions were incubated for one hour, then removed and the surface wettability tested with 1 ml of autoclaved deionized water (see also Supplemental Movie 1). Note that only heparin can convert the hydrophobic plastic into a hydrophilic surface. ASWH, artificial sea water buffered with HEPES, scale bar: 1 cm.

Suppl. Figure 4. DOPA presence in test cells at the one cell stage.

(A-C') Double fluorescence of anti-DOPA antibody with nuclear DAPI and (D-D') DOPA-NBT staining on one cell stage embryos. (A,A') confocal projection of anti-DOPA staining and (B, B') DAPI staining (C,C') overlay of double fluorescence with DIC image. (D,D') DIC image of DOPA-NBT staining (purple). The areas of enlargement is indicated with a rectangle, arrowheads indicate three individual test cells. FC, follicle cells surrounding the test cells. Scale bars: (A-D) 25 μ m, (A-D') 5 μ m.

Suppl. Figure 5. DOPA presence in test cells of hatching larvae.

(A, A') Anti-DOPA antibody fluorescent staining and (B) DOPA-NBT staining of hatching larvae. (A') Anti-DOPA antibody (green) fluorescence and (B) NBT staining (purple) on hatching larvae overlaps with test cells (arrowheads) on the tunic surrounding the larval trunk. Anterior is to the left, arrows mark the papillae. Scale bar: 25 μ m.

Supplemental Table. Surface characterization data, showing advancing and receding contact angles, and ellipsometric thicknesses for the SAMs.

SAM	Advancing contact angle (deg)	Receding contact angle (deg)	Ellipsometric thickness (\AA)
C16	110 \pm 1	106 \pm 1	20.4 \pm 0.8
MHA	33 \pm 2	< 10	23.0 \pm 0.5
NH2	35 \pm 2	< 10	21.6 \pm 0.8
EG6	37 \pm 2	23 \pm 1	37.2 \pm 0.7

Supplemental Movie 1: Heparin mediated surface wettability.

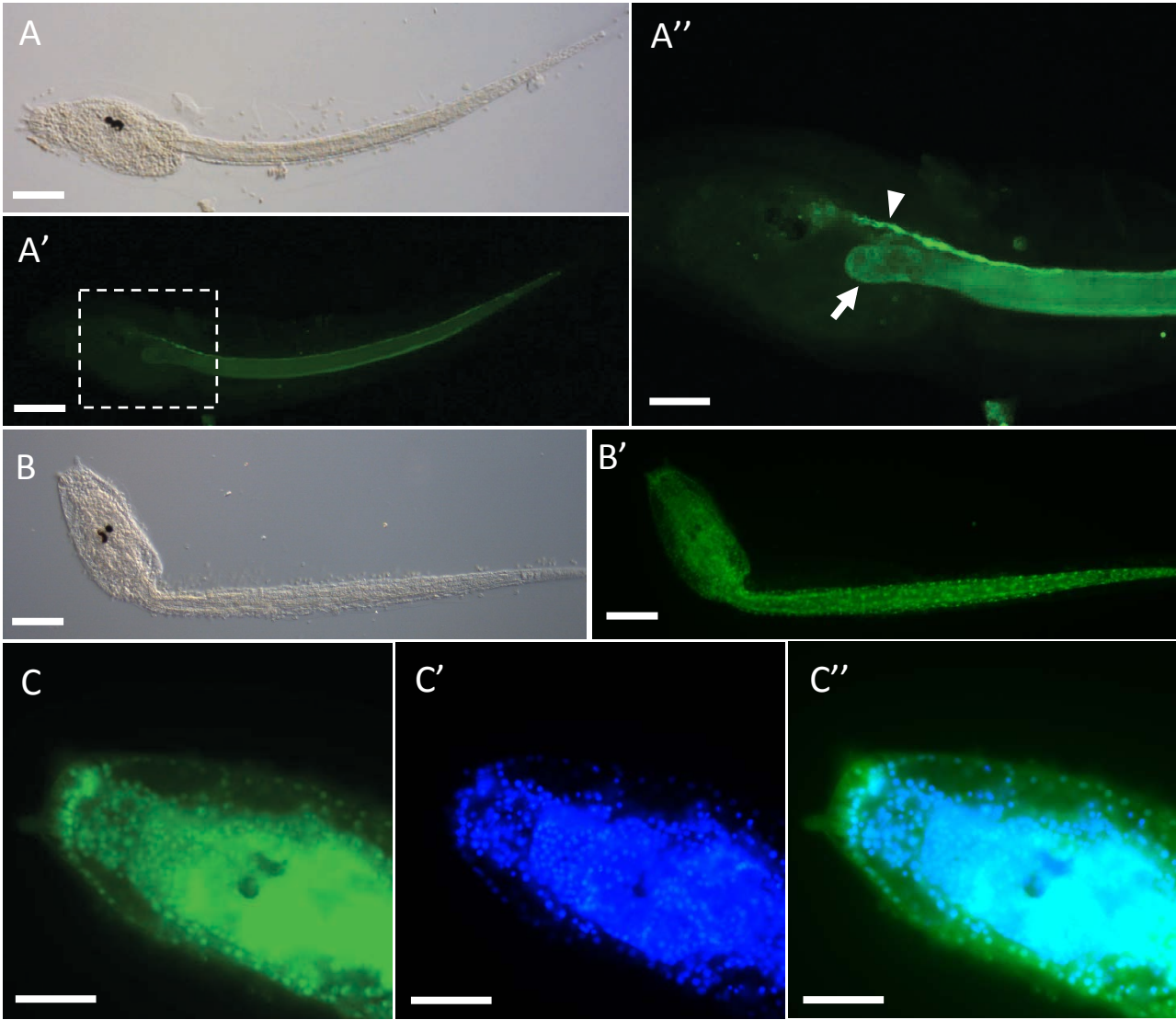
The surface wettability is tested with 1 ml of autoclaved deionized water after having incubated the Petri dishes for one hour and removed the indicated solutions: ASWH, or heparin, glutamic acid and aspartic acid (each 2.5% in ASWH).

Supplemental Movie 2: DOPA presence in papillae and test cells. Double fluorescent labelling with (green) anti-DOPA-antibody and (blue) nuclear DAPI (as in Fig. 5h) are shown as a series of individual confocal images of 0.5 μ m optical z-sections.

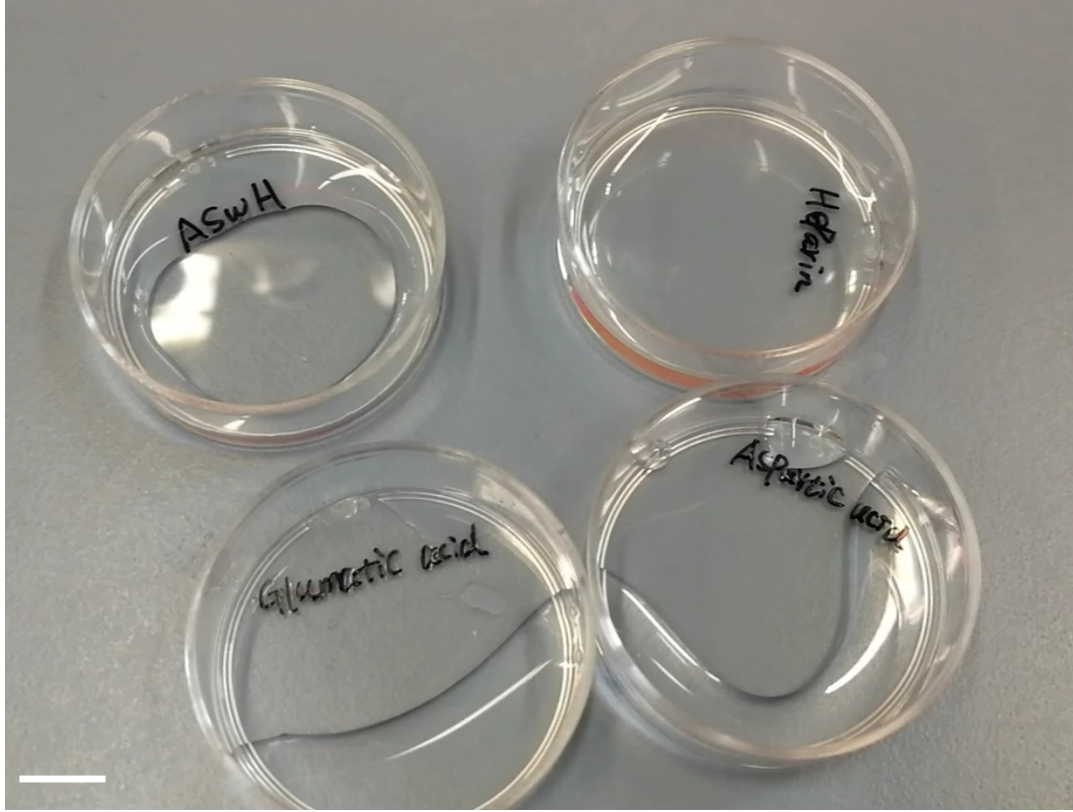
Suppl. Fig. 1



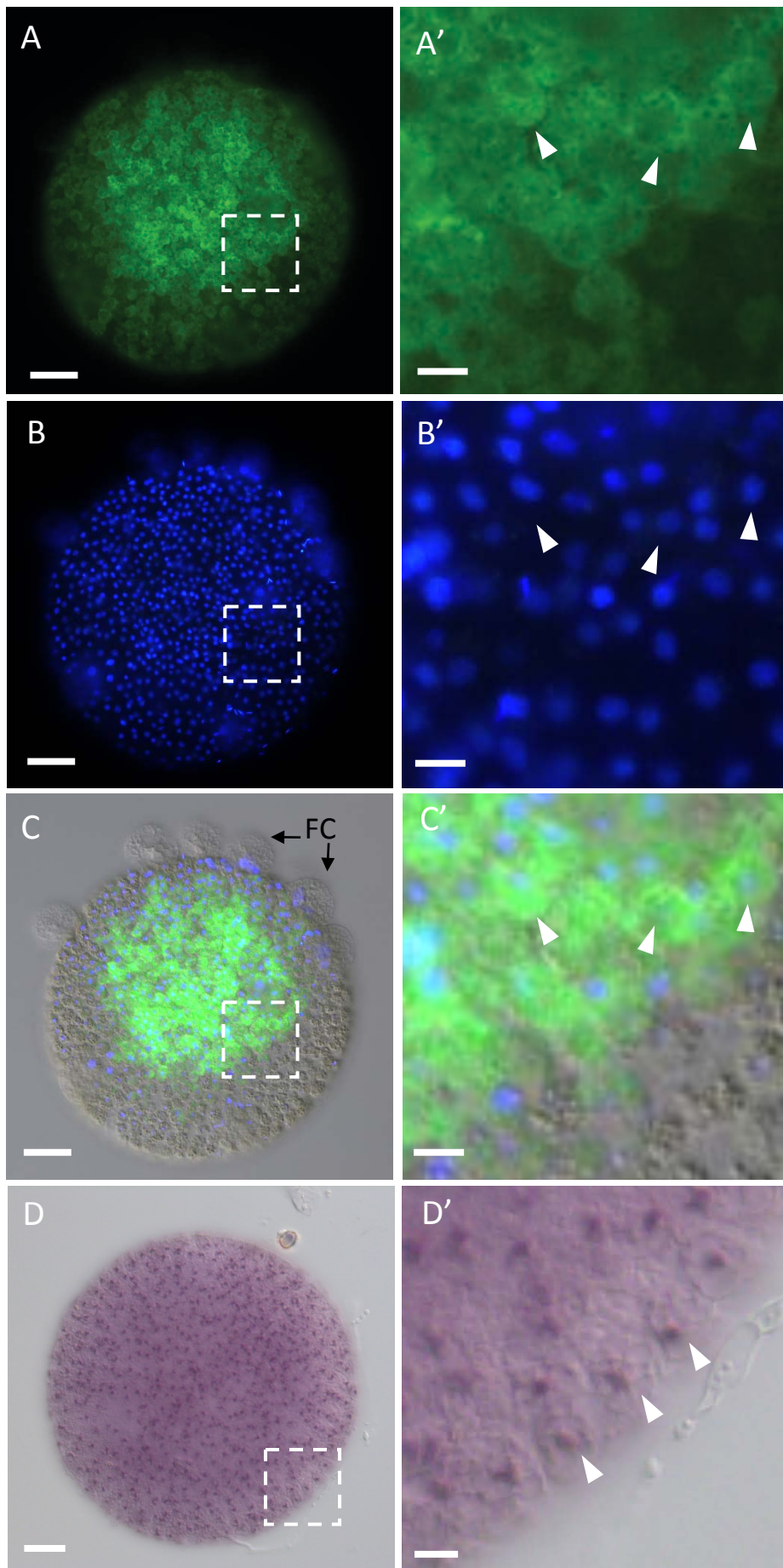
Suppl. Fig. 2



Suppl. Fig. 3



Suppl.
Fig. 4



Suppl. Fig. 5

